

# Reclamation of used SiC grinding powder and its sintering characteristics

Ningfeng Gao<sup>a,b,\*</sup>, Koji Watari<sup>a</sup>, Shoichi Kume<sup>a</sup>, Yukari Ando<sup>b</sup>, Sasai Ryo<sup>b</sup>, Hideaki Itoh<sup>b</sup>

<sup>a</sup> National Institute of Advanced Industrial Science and Technology (AIST), Advanced Manufacturing Research Institute, 2266-98 Aanagahora, Shimoshidami, Moriyama-ku, Nagoya 463-8560, Japan

<sup>b</sup> EcoTopia Science Institute, Nagoya University, Furocho, Chikusa-ku, Nagoya 464-8603, Japan

Available online 10 August 2005

## Abstract

A process of recycling used abrasive SiC powder after grinding Si wafer was proposed to raw powder for sintering. The used SiC powder could be successfully converted to composite powders consisting of SiC particle and Si<sub>3</sub>N<sub>4</sub> whisker via a heat treatment in N<sub>2</sub> atmosphere, in which iron oxide acted as a catalyst in the vapor–liquid–solid (VLS) formation of Si<sub>3</sub>N<sub>4</sub>. With the addition of 3 mass% Al<sub>2</sub>O<sub>3</sub> and 1 mass% Y<sub>2</sub>O<sub>3</sub>, the composite powders sintered at 1900 °C for 2 h exhibited a 3-point bending strength of 626 ± 48 MPa and a fracture toughness of 3.9 ± 0.1 MPa m<sup>1/2</sup>, which were significantly enhanced as compared with those of using recovered powder merely composed of SiC particle. The strength and fracture toughness of the sintered material could be improved by optimization of chemical and heat treatment parameters and controlling the amount of sintering additives and hot pressing conditions.

© 2005 Elsevier Ltd. All rights reserved.

**Keywords:** SiC; Recycling; Sintering; Mechanical properties; Microstructure-final

## 1. Introduction

SiC ceramic has many engineering applications such as machining tool, abrasive material, heat resisting structural material, power semiconductor and so on, due to its high mechanical and thermal properties. There are mainly two methods to synthesize SiC powder industrially. The first method is called Acheson process, which employs direct carburization of silica at firing temperature of 2000–2200 °C. The second method is direct reduction of metallic silicon at the temperature of 1400–1800 °C, which is suitable to fabricate much purer SiC used in the semiconductor industry.<sup>1</sup> Due to the high processing temperature of 1400–2200 °C, the high cost and the high environmental load are problematic. Therefore, it is of great significance to recycle the SiC for the sake of lowering the overall cost and environmental load.

There are seldom reports concerning the recycling of SiC ceramic to the best of our knowledge. A study on the recycling of used silicate bonded SiC refractory has been reported, in which bauxite and silica fume were added to the SiC-based

refractory so as to transform it to SiC–mullite composites at the firing temperature of 1400 °C.<sup>2</sup> In the application area of using SiC as abrasive material, the yearly production has reached 1959 ton in Japan, most of which are discarded after usage.<sup>3</sup> The current study was focused on the reclamation of abrasive SiC powder discharged from the semiconductor industry. After services for polishing Si wafer, exfoliated Si scraps were introduced into the abrasive powder and Fe impurity also existed originating from the fabrication process of the grinding powder. Due to reduction of SiC particle size, change of particle size distribution and shape, which led to varied viscosity of grinding slurry and unstable performance, it is difficult to reuse the SiC as grinding powder.<sup>4</sup>

In this study, a process of recycling the used SiC powder was proposed from a viewpoint of cascade recycling. The inclusion of Si content in the used SiC powder was undesirable and had to be eliminated before sintering. It is widely known that the sintered monolithic SiC usually had a low fracture toughness and reinforcement of SiC with Si<sub>3</sub>N<sub>4</sub> whisker is a feasible process to improve the fracture toughness of SiC due to the crack deflection and bridging, and pull-out effect of whiskers.<sup>5</sup> The presence of Si content in the used SiC powder makes it possible to take advantage of nitridation of

\* Corresponding author. Tel.: +81 996 20 1836.

E-mail address: [nfgaojp@yahoo.co.jp](mailto:nfgaojp@yahoo.co.jp) (N. F. Gao).

the Si content to  $\text{Si}_3\text{N}_4$  whisker in situ. The nitridation product of  $\text{Si}_3\text{N}_4$  whisker may serve as a reinforcement phase in the SiC matrix. Consequently, this work aims to evaluate the possibility of transforming the used SiC powder to composite powders with whisker reinforcement and investigates the sintering characteristics of the nitrated composite powders.

## 2. Experimental procedure

Used SiC powder for grinding Si wafer was provided by Sanwayuka Kogyo Co., Japan. The powder for sintering was pulverized by ball milling before heat treatments in a tube furnace with  $\text{N}_2$  flow of 30 ml/min to produce  $\text{Si}_3\text{N}_4$  whisker. The temperature was raised to 900–1400 °C at a rate of 2.5 °C/min and kept for 0–4 h. Some powder samples were pre-treated at 500 °C for 0.5 h in air to eliminate organic impurities originating from slurry. The contents of organic impurities were measured by a carbon, hydrogen and nitrogen determinator (MT-6, Yanaco Bunseki Kogyo Co., Japan). For comparison some powder samples for sintering were also hydrothermally treated in 1 M NaOH or 1 M HCl solution so as to dissolve the Si or Fe impurity. The amounts of Si and Fe contained in the used SiC powder were calculated from the ion concentration in the filtrate measured by inductively coupled plasma-atomic emission spectrometry (ICP-AES). The average particle size was calculated from BET surface area.

The nitrated powders were composed of SiC particle (hereafter denoted as  $\text{SiC}_p$ ) and  $\text{Si}_3\text{N}_4$  whisker (hereafter denoted as  $\text{Si}_3\text{N}_{4w}$ ).  $\text{Al}_2\text{O}_3\text{--Y}_2\text{O}_3$  (2 or 4 mass%; hereafter denoted as AlYO) and sintering additives (mass ratio of  $\text{Al}_2\text{O}_3\text{:Y}_2\text{O}_3 = 3\text{:}1$ ) were mixed with the composite powders by sonication in ethanol. Then the starting powder mixtures were uniaxially compacted to a rectangular shape of 30 mm × 40 mm × 8 mm. The rectangular green body was subsequently put into a graphite die with BN powder bed acting as a media for the transferring of pressure in hot pressing. The hot pressing parameters were temperature of 1900 °C, pressure of 40 MPa, duration of 2 h and atmosphere of 0.3 atm Ar.

The density and open porosity were determined by Archimedes method using water immersion. Microstructure observation was performed by a scanning electron microscope (SEM) equipped with an energy dispersive spectrometer (EDS). Phase compositions were determined by X-ray diffraction (XRD) using  $\text{Cu K}\alpha$  irradiation. The phases and grain boundary structure of the sintered bodies were investigated in detail by transmission electron microscope (TEM, JEM-2010, JEOL Co., Japan) combined with an EDS. The Vickers hardness was measured at an indentation load of 98 N. The value of 3-point bending strength was an average of at least four samples with the cross section of 3 mm × 4 mm at a span of 30 mm. Fracture toughness measurement was conducted using single edge notched beam (SENB) in accordance with Japanese Industrial Standard (JIS) 1607.

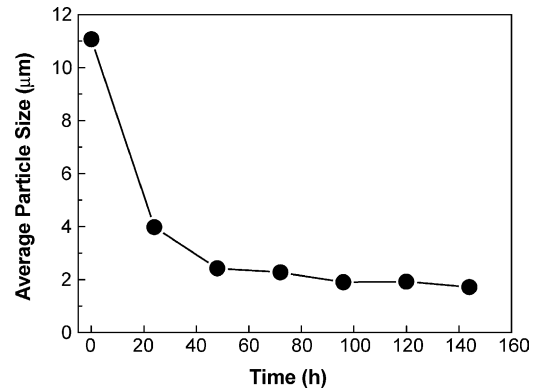


Fig. 1. Average particle size of the used SiC powder as a function of treatment time after ball milling pulverization.

## 3. Results and discussion

### 3.1. Characterization of used SiC powder and pulverization effect by ball milling

The measurement using carbon, hydrogen and nitrogen determinator showed that the organic content in the used SiC powder was 4.9 mass%, which was made up of 4.3 mass% C and 0.6 mass% H. After usage, the average particle size of the used SiC powder was reduced to 11 from 18 μm of the virgin SiC. In addition, particle size distribution as measured by a laser diffraction and scattering particle size analyzer showed the existence of particles with sizes in the range of 0.1–1 μm. This could be attributed to the fine Si and SiC scraps. Ball milling using  $\text{Si}_3\text{N}_4$  balls in ethanol was carried out to pulverize the used SiC powder. The mass ratio of balls to powder mixtures was around 8. Fig. 1 illustrates the change of average particle size as a function of ball milling time. A duration of 144 h could effectively reduce the particle size to an average of 2 μm. After nitridation treatment the ball milled powder was sintered by hot pressing in Ar atmosphere.

### 3.2. Nitridation of used SiC powder

#### 3.2.1. Characterization of nitrated SiC powder

Fig. 2 shows the SEM micrographs of the used SiC powder before and after a nitridation treatment at 1300 °C for 1 h. Some fiber-like particles were observed on the surface of the nitrated powders with diameters of 0.1–0.2 μm and lengths longer than 10 μm. This kind of fiber-like particle is usually observed in powder treated above 1000 °C. Fig. 3 shows the corresponding XRD patterns of the SiC powders before and after nitridation. It can be seen that the peaks attributed to Si disappeared from the used SiC powder, while small  $\alpha\text{-Si}_3\text{N}_4$  peaks in the  $2\theta$  range of 20–27° emerged after the nitridation treatment. The synthesized fiber-like particles showing a discernible white color could be easily separated from the green SiC powder. The XRD analysis on the collected fiber-like particles from the reaction crucible revealed only the diffraction peaks from  $\alpha\text{-Si}_3\text{N}_4$ . TEM micrograph and the corresponding

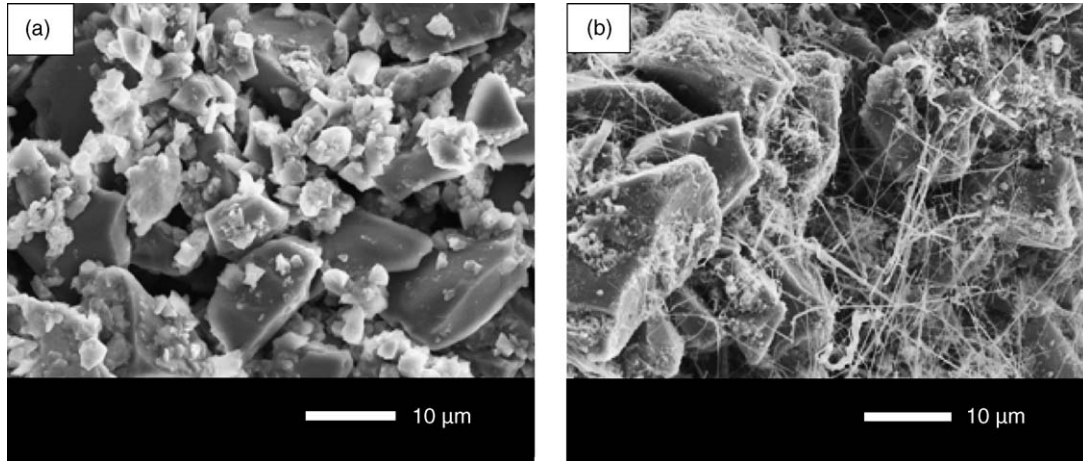


Fig. 2. SEM micrographs of the used SiC powder before (a) and after a nitridation treatment at 1300 °C for 1 h (b). The used SiC powder was not pulverized before nitridation.

selected area electron diffraction (SAED) pattern as shown in Fig. 4 confirmed that the fiber-like particle was single crystalline  $\alpha$ - $\text{Si}_3\text{N}_4$  with hexagonal structure. There were seldom crystal defects in the whisker. The  $\alpha$ - $\text{Si}_3\text{N}_{4w}$  with length as

long as 100 μm and aspect ratio higher than 500 had also been observed by TEM.

3.2.2. Optimization of nitridation conditions and reaction mechanisms

The nitridation process was carried out at 900–1400 °C for 0–3 h in  $\text{N}_2$  flow. The nitrided powders were immersed in 1 M NaOH solution to dissolve Si and the amount of unreacted Si was calculated from the Si ion concentration in the filtrate.

Fig. 5 demonstrates the  $\text{Si}_3\text{N}_4$  production rate as a function of duration at various treatment temperatures. The  $\text{Si}_3\text{N}_4$  production rate from Si impurity was estimated from the amount of unreacted Si after nitridation process. At a fixed duration of 1 h,  $\text{Si}_3\text{N}_4$  production rate was low at 1000 °C and increased with the increasing temperature to 1400 °C, reaching a value of 99%. The nitridation at 1400 °C for 1 h was enough to convert nearly all the Si content to  $\text{Si}_3\text{N}_4$ , which was employed to process the starting powder for hot-press sintering.

The notable formation of  $\text{Si}_3\text{N}_{4w}$  could only be observed by SEM in the nitrided powders above 1100 °C. At 1000 and 1100 °C, the extension of nitridation duration did not lead to remarkable increase of the  $\text{Si}_3\text{N}_4$  production rate. It is evident

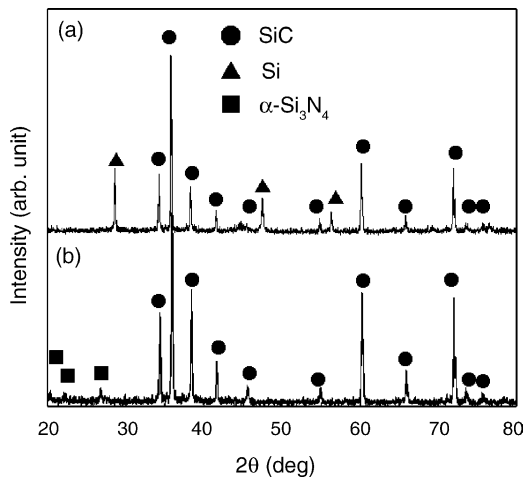


Fig. 3. XRD patterns of the used SiC powder before (a) and after a nitridation treatment at 1300 °C for 1 h (b).

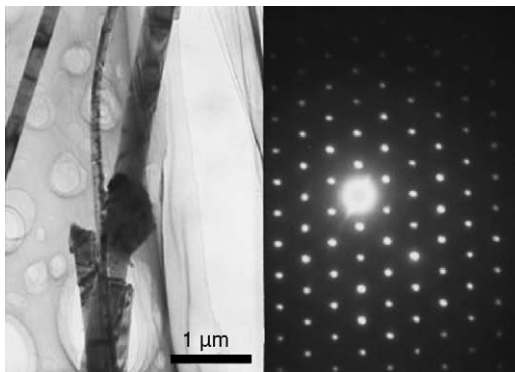


Fig. 4. TEM micrograph of the fiber-like grain and the corresponding SAED pattern of  $\alpha$ - $\text{Si}_3\text{N}_4$ . The direction of the incident electron is [0 0 1].

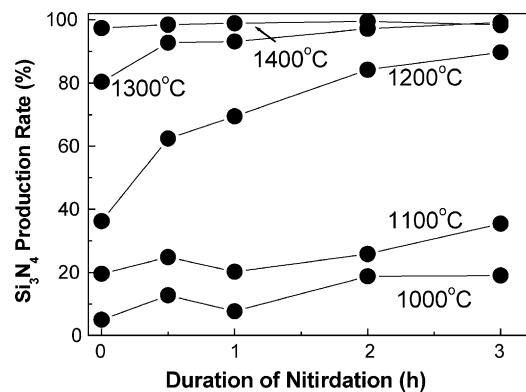


Fig. 5. Variation of  $\text{Si}_3\text{N}_4$  production rate with the duration of nitridation treatment at various temperatures.

that there is a conspicuous change in the production rate at the temperature between 1100 and 1200 °C. The morphology of the produced  $\text{Si}_3\text{N}_{4w}$  nitrided at 1000–1100 °C was short fiber with diameter less than 0.2  $\mu\text{m}$  stretching out from the surface of Si or SiC.

However, with the increasing of treatment temperature to 1200–1400 °C, the whisker produced showed not only the morphology of short fiber but also long and thick fiber with diameter more than 0.5  $\mu\text{m}$ . SEM observation at higher magnification showed the frequent presence of spherical particle at the tip of the long and thick whisker, which was likely a product of a liquid reaction. The EDS elemental mapping revealed that the spherical particle was abundant in Fe and O. The O in the reaction system may originate from the oxidized surface of Si and SiC or the  $\text{Al}_2\text{O}_3$  crucible. It is widely known that there is a eutectic reaction to form  $\text{FeSi}_2$  in the Si rich region of the Fe–Si binary system at 1212 °C.<sup>6</sup> The addition of O into the Fe–Si binary system may further reduce the liquid reaction temperature. The isothermal section of FeO– $\text{Fe}_2\text{O}_3$ – $\text{SiO}_2$  system at 1300 °C showed that in all the Si rich regions, liquid phase formed, which was in equilibrium with wustite (FeO), magnetite ( $\text{Fe}_3\text{O}_4$ ), Fe or  $\text{SiO}_2$ .<sup>7</sup> It is, therefore, suggested that the formation of  $\alpha$ - $\text{Si}_3\text{N}_4$  above 1200 °C was mainly through a VLS mechanism with the iron oxide acting as a catalyst.<sup>8,9</sup> At the initial stage of nitridation Fe contacting with Si or SiC reacted to form a liquid phase of Fe–Si–O compositions. With continuous feeding of  $\text{N}_2$  gas,  $\text{N}_2$  dissolved in the liquid droplet to the saturated concentration level, which brought about the nucleation and growth of  $\alpha$ - $\text{Si}_3\text{N}_4$  from the liquid droplet. As the whisker was growing, the liquid droplet was lifted up. The grain growth may stop until all the Si specie in the liquid was consumed and leaving the Fe–O spherical grain at the tip of  $\alpha$ - $\text{Si}_3\text{N}_{4w}$ . In order to clarify the role of the Fe in the nitridation process, the Fe content in some powder SiC samples was removed by a hydrothermal treatment in 1 M HCl solution at 200 °C for 24 h. The removal of Fe resulted in the reducing of the  $\text{Si}_3\text{N}_4$  production rate from 93 to 58% when the powder was nitrided at 1300 °C for 1 h.

At lower temperature of 1000–1100 °C the reaction may be dominated by a vapor–solid (VS) reaction, in which  $\text{Si}_3\text{N}_4$  was suggested, to form by the reaction between the intermediate phase of SiO and  $\text{N}_2$  gas. The resulting product was short whisker with diameter less than 0.2  $\mu\text{m}$ . The possibility for the partial formation of amorphous  $\text{SiO}_2$  fiber could almost be ruled out due to the existence of iron oxide as a catalyst in the present study.<sup>10</sup>

### 3.3. Sintering characteristics of nitrided SiC powder

#### 3.3.1. Physical properties of the sintered bodies

AlYO sintering additives were added to the nitrided powders in order to sinter SiC in the presence of liquid phase. It has been reported that the highest density of SiC could be achieved at the  $\text{Y}_2\text{O}_3$  content of 25–40 mass% of the total AlYO additives in the pressureless sintering of SiC at 1800–2000 °C.<sup>11</sup> In the present study the mass ratio of  $\text{Al}_2\text{O}_3$ : $\text{Y}_2\text{O}_3$  was also fixed at 3:1 (25 mass%  $\text{Y}_2\text{O}_3$ ). Generally, the Fe in the nitrided powders was not removed before hot-press sintering in respect of lowering the overall recycling cost.

Table 1 lists the physical and mechanical properties of the hot-press sintered compacts at 1900 °C, 40 MPa for 2 h. Because the phase compositions of the sintered bodies were very complicated, the theoretical density of 6H–SiC (3.20  $\text{g cm}^{-3}$ ) was assumed to be the theoretical value of the sintered bodies in the calculation of the relative density. It is obvious that the nitrided composite powders were more easily densified and thus both the strength and toughness of sample A increased as compared to sample B. Sample C exhibited the most excellent mechanical properties among all the samples. With the addition of 4 mass% AlYO sintering additives, the composite powder mixtures sintered at 1900 °C for 2 h showed a 3-point bending strength of  $626 \pm 48$  MPa and a fracture toughness of  $3.9 \pm 0.1$   $\text{MPa m}^{1/2}$ , which were enhanced by a ratio of 105% and 22% as compared to those of using un-nitrided SiC powder for sample B, respectively. On the other hand, the sample C demonstrated almost the same fracture toughness but a much higher bending strength as compared to sample A. SEM observation on the polished surface of samples A and C revealed almost the same grain and pore structures. The difference of the bending strength for samples A and C is likely attributable to the stronger bonding of intergranular crystalline phase for sample C, which fractured in a transgranular mode in contrary to an intergranular mode for sample A from SEM observation.

Zhou et al. investigated the mechanical properties of highly pure and fine-grained sintered 3C–SiC with an average grain size of 0.78  $\mu\text{m}$ . The sintered body with 98.5% theoretical density demonstrated a bending strength of  $587 \pm 48$  MPa, fracture toughness of  $3.7 \pm 0.2$   $\text{MPa m}^{1/2}$  and hardness of  $19.7 \pm 0.4$  GPa with the addition of 5 mass% AlYO additives.<sup>12</sup> The mechanical properties obtained for sample C in this study are even superior to the above reported values. Further enhancement of the mechanical properties for

Table 1  
Comparison of the physical and mechanical properties of the sintered SiC hot-pressed at 1900 °C, 40 MPa for 2 h

| Sample number | Starting powders   | Bending strength (MPa) | Fracture toughness ( $\text{MPa m}^{1/2}$ ) | Vickers hardness (GPa) | Bulk density ( $\text{g cm}^{-3}$ ) | Open porosity (%) | Relative density (%) |
|---------------|--|------------------------|---|------------------------|-------------------------------------|-------------------|----------------------|
| A             | $\text{SiC}_p + \text{Si}_3\text{N}_{4w} + 2$ mass% AlYO | $340 \pm 44$           | $3.8 \pm 0.2$                               | $15.3 \pm 1.5$         | 3.04                                | 2.2               | 95.1                 |
| B             | $\text{SiC}_p + 2$ mass% AlYO                            | $306 \pm 39$           | $3.2 \pm 0.4$                               | $20.7 \pm 1.3$         | 2.92                                | 6.3               | 91.4                 |
| C             | $\text{SiC}_p + \text{Si}_3\text{N}_{4w} + 4$ mass% AlYO | $626 \pm 48$           | $3.9 \pm 0.1$                               | $19.7 \pm 1.0$         | 3.14                                | 0.5               | 98.0                 |



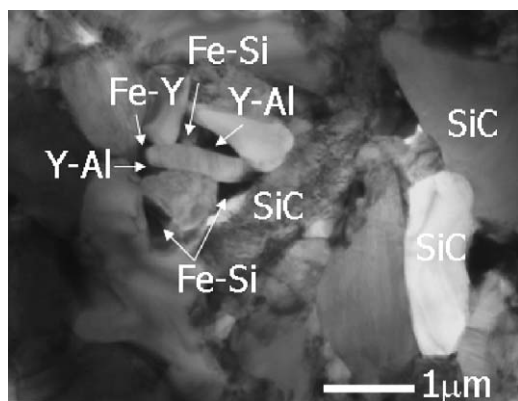


Fig. 6. TEM micrograph of the sintered SiC hot-pressed at 1900 °C for 2 h. The compositions of the starting powder mixtures were  $\text{SiC}_p + \text{Si}_3\text{N}_{4w} + 4 \text{ mass\% AIYO}$ .

the sintered SiC powder could be expected by taking some measures such as removal of Fe impurity in  $\text{Si}_3\text{N}_{4w}$  and optimization of sintering parameters.

### 3.3.2. Phase compositions and microstructure characterization

Fig. 6 shows the TEM micrographs of sample C. The sintered body showed a dense microstructure corresponding to a relative density of 98.0% and an open porosity of 0.5% as listed in Table 1. The sintered body mainly consisted of equiaxial SiC grains with some plate-like or rod-shaped SiC grains, which were not observed in the case using un-nitrided SiC powder. The plate-like or rod-shaped grains may contribute to the high fracture toughness for sample C. The elements contained in the sintering additives and the Fe impurity mainly existed in the triple junction points or the triple pocket structures. Maximum solubility of 4 at.% Al and 3 at.% O were detected in SiC grains by EDS. The elemental compositions in the three junction points or the pocket structures could be divided into three categories, which are mainly composed of Fe–Si, Y–Al and Fe–Y as indicated in the TEM micrograph. The Fe–Si composition corresponded to the  $\text{FeSi}_2$ –Si eutectic point, while Y–Al area consisted of glassy phase or crystallized yttrium aluminum garnet (YAG).

Fig. 7 plots the XRD patterns of samples sintered at 1900 °C for 2 h. 6H–SiC and YAG were two-phase components detected in all the sintered samples. Si emerged as a result of the decomposition of  $\text{Si}_3\text{N}_{4w}$  for samples A and C. Due to the overlap of the main diffraction peaks of YAG,  $\alpha$ - $\text{Si}_3\text{N}_4$ ,  $\alpha$ -Sialon and AlN, it is hard to determine the existence of  $\alpha$ - $\text{Si}_3\text{N}_4$ ,  $\alpha$ -Sialon and AlN in the sintered bodies only from the XRD patterns. High resolution TEM observation detected some rod-shaped AlN-polytypoid grains in sample C. The EDS analysis revealed that a small amount of Mg was also incorporated into the AlN-polytypoid. The formation of AlN-polytypoid could not only reduce the amount of grain boundary glassy phase but increase the high temperature mechanical properties as well.<sup>13,14</sup>

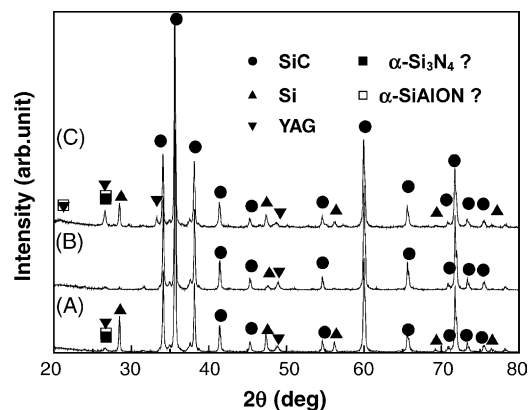


Fig. 7. XRD patterns of the sintered SiC samples hot-pressed at 1900 °C for 2 h. The compositions of the starting powder mixtures were  $(\text{SiC}_p + \text{Si}_3\text{N}_{4w} + 2 \text{ mass\% AIYO})$  (A),  $(\text{SiC}_p + 2 \text{ mass\% AIYO})$  (B),  $(\text{SiC}_p + \text{Si}_3\text{N}_{4w} + 4 \text{ mass\% AIYO})$  (C), respectively.

The sintered SiC using the nitrided powder has the potentials to be used as fire resistant material, high temperature structural material and material for heating element. The recycling of the used SiC abrasive powder to raw material for sintering is a process of low cost and energy saving, which can lower the environmental load of the used SiC waste.

## 4. Conclusions

A new process of recycling the used SiC powder for grinding Si wafer to raw powder was put forward in the present study. The used SiC powder could be successfully converted to composite powders consisting of  $\text{SiC}_p$  and  $\alpha$ - $\text{Si}_3\text{N}_{4w}$  via a heat treatment in  $\text{N}_2$  atmosphere at 1400 °C for 1 h. Iron oxide acted as a catalyst in the formation of  $\alpha$ - $\text{Si}_3\text{N}_4$  at the nitridation temperature of 1200–1400 °C via a VLS mechanism. The formation of  $\alpha$ - $\text{Si}_3\text{N}_{4w}$  at the nitridation temperature of 1000–1100 °C was controlled by a VS mechanism. With the addition of 4 mass% AIYO sintering additives, the nitrided powder sintered at 1900 °C for 2 h exhibited a 3-point bending strength of  $626 \pm 48 \text{ MPa}$  and a fracture toughness of  $3.9 \pm 0.1 \text{ MPa m}^{1/2}$ , which were significantly enhanced as compared to those of using un-nitrided powder.

## References

- Suzuki, H., Iseki, T. and Tanaka, H., *Advance Silicon Carbide Ceramics*. Uchida Rokakuho Publishing, Tokyo, 2001, pp. 119–127.
- Ewais, E. M. M., Al-Wakeel, M. I., Khalil, N. and Ahmed, Y. M. Z., New refractories made from reused silicon carbide. *J. Ceram. Sci. Jpn.*, 2004, **112**, 428–433.
- Yamazaki, M., Industrial trend and statistics of artificial abrasives. *Ceram. Jpn.*, 2003, **38**, 730–731.
- Ando, Y., Sasai, R. and Itoh, H., Recycling of used abrasive powder of SiC by hydrothermal treatment. *Abstract book of Annual Meeting of the Ceramic Society of Japan*. Ceramic Society of Japan, Tokyo, 2002, p. 198.

5. Liang, Y. N., Lee, S. W. and Park, D. S., Effects of whisker distribution and sintering temperature on friction and wear of  $\text{Si}_3\text{N}_4$ -whisker-reinforced  $\text{Si}_3\text{N}_4$ -composites. *Wear*, 1999, **225–229**, 1327–1337.
6. Baker, H., Alloy phase diagrams. *ASM Handbook*. ASM International, Ohio, 1992, p. 2.203.
7. Fabrichnaya, O. B. and Sundman, B., The assessment of thermodynamic parameters in the Fe–O and Fe–Si–O systems. *Geochim. Cosmochim. Acta*, 1997, **21**, 4539–4555.
8. Kawai, C. and Yamakawa, A., Crystal growth of silicon nitride whiskers through a VLS mechanism using  $\text{SiO}_2$ – $\text{Al}_2\text{O}_3$ – $\text{Y}_2\text{O}_3$  oxides as liquid phase. *Ceram. Int.*, 1997, **24**, 135–138.
9. Silva, P. C. and Figueiredo, J. L., Production of SiC and  $\text{Si}_3\text{N}_4$  whisker in C+ $\text{SiO}_2$  solid mixtures. *Mater. Chem. Phys.*, 2001, **72**, 326–331.
10. Zhang, Y. J., Wang, N. L., He, R. R., Liu, J., Zhang, X. Z. and Zhu, J., A simple method to synthesize  $\text{Si}_3\text{N}_4$  and  $\text{SiO}_2$  nanowires from Si or Si/ $\text{SiO}_2$  mixture. *J. Crystal Growth*, 2001, **233**, 803–808.
11. Mushtaq, Q. and Kristic, V. D., Low-temperature pressurless sintering of  $\beta$ -silicon carbide with aluminum oxide and yttrium oxide additions. *Ceram. Bull.*, 1991, **70**, 439–443.
12. Zhou, Y., Hirao, K., Toriyama, M., Yamauchi, Y. and Kanzaki, S., Effects of intergranular phase chemistry on the microstructure and mechanical properties of silicon carbide ceramics densified with rare-earth oxide and alumina additions. *J. Am. Ceram. Soc.*, 2001, **84**, 1642–1644.
13. Wang, P. L., Zhang, W. Y., Sun, W. Y. and Yan, D. S., Formation behavior of multi-cation  $\alpha$ -sialons containing calcium and magnesium. *Mater. Lett.*, 1999, **38**, 178–185.
14. Wang, P. L., Sun, W. Y. and Yan, D. S., Mechanical properties of AlN-polytypoids—15R, 12H and 21R. *Mater. Sci. Eng. A*, 1999, **272**, 351–356.